

A New Type of Charge-Transfer Salts Based on Tetrathiafulvalene–Tetracarboxylate Coordination Polymers and Methyl Viologen

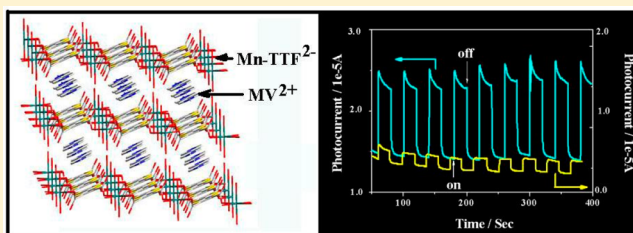
Yu-De Huang,[†] Peng Huo,[†] Ming-Yan Shao,[†] Jing-Xue Yin,[†] Wei-Chun Shen,[†] Qin-Yu Zhu,^{*,†,‡} and Jie Dai^{*,†,‡}

[†]College of Chemistry, Chemical Engineering and Materials Science, Soochow University, Suzhou 215123, People's Republic of China

[‡]State Key Laboratory of Coordination Chemistry, Nanjing University, Nanjing 210093, People's Republic of China

Supporting Information

ABSTRACT: Although charge-transfer compounds based on tetrathiafulvalene (TTF) derivatives have been intensively studied, $\{[\text{cation}]^{n+} \cdot [\text{TTFs}]^{n-}\}$ ion pair charge-transfer (IPCT) salts have not been reported. The aim of this research is to introduce functional organic cations, such as photoactive methyl viologen (MV^{2+}), into the negatively charged TTF–metal coordination framework to obtain this new type of IPCT complex. X-ray structural analysis of the four compounds $(\text{MV})_2[\text{Li}_4(\text{L})_2(\text{H}_2\text{O})_6]$ (1), $\{(\text{MV})(\text{L})[\text{Na}_2(\text{H}_2\text{O})_8] \cdot 4\text{H}_2\text{O}\}_n$ (2), $\{(\text{MV})[\text{Mn}(\text{L})(\text{H}_2\text{O})_2] \cdot 2\text{H}_2\text{O}\}_n$ (3), and $\{(\text{MV})[\text{Mn}(\text{L})(\text{H}_2\text{O})_2]\}_n$ (4), reveals that the electron donor (D) TTF moiety and the electron acceptor (A) MV^{2+} form a regular mixed-stack arrangement in alternating DADA fashion. The TTF moiety and the MV^{2+} cation are essentially parallel stacked to form the column structures. The strong electrostatic interaction is a main force to shorten the distance between the cation and anion planes. Optical diffuse-reflection spectra indicate that charge transfer occurs in these complexes. The ESR and magnetic measurements confirm that there is strong charge-transfer-induced partial electron transfer. Compounds 2, 3, and 4 show an effective and repeatable photocurrent response. The current intensities of 3 and 4 are higher than that of 2, which reflects that the coordination center of the Mn(II) ion has a great effect on the increasing photocurrent response.



INTRODUCTION

Charge-transfer materials have gathered immense attention due to their versatile electronic functionalities and applications that result from the ground-state electron transfer between electron donor (D) and electron acceptor (A) moieties.¹ The first reported metallic charge-transfer (CT) salt is formed by tetrathiafulvalene (TTF) and tetracyanoquinodimethane (TCNQ),² in which TTF acts as an electron-rich donor. By using the unique property of the TTF moiety, TTF and its derivatives (TTFs) have been successfully used as building blocks for the formation of charge-transfer compounds, giving rise to organic conductors and even superconductors.³ Various TTF-related D–A compounds have been investigated in these decades for studies of molecular-level devices,^{4,5} such as molecular switches and sensors.

Most of these molecules are covalently linked D–A compounds, including D–A diads and D–A–D/A–D–A triads. Charge-transfer salts formed between cations and anions (i.e., ion pair charge-transfer, IPCT, complexes) are among an interesting subclass of the D–A system.⁶ A series of $\{[\text{TTFs}]^{n+} \cdot [\text{anion}]^{n-}\}$ charge-transfer salts have been reported.^{3,7} The other type of IPCT complex $\{[\text{cation}]^{n+} \cdot [\text{TTFs}]^{n-}\}$, to the best of our knowledge, has not been reported yet, because the TTF moiety is usually neutral and can be oxidized only to the corresponding radical cation and dication. The key to obtain

the $\{[\text{cation}]^{n+} \cdot [\text{TTFs}]^{n-}\}$ IPCT complexes is apparently that negative charge should be introduced to the TTF moiety. The advantage of such complexes is that functional organic cations are able to be introduced into IPCT compounds of TTF.

We and other groups have reported a series of metal coordination complexes of TTF–carboxylates with transition metal ions^{8,9} and supramolecular salts with alkaline metal cations.^{10,11} The TTF–carboxylates can be used as building blocks to construct multidimensional frameworks with various $\pi \cdots \pi$ interactions, short contacts, and hydrogen bonds. The negatively charged TTF–carboxylates are a kind of unique TTF derivatives that motivated us to synthesize the unknown $\{[\text{cation}]^{n+} \cdot [\text{TTFs}]^{n-}\}$ IPCT complexes. On the other hand, although charge-transfer salts of TTFs have attracted considerable attention, few charge-transfer salts constructed by TTF coordination polymers have been reported so far. Our strategy is to integrate a negatively charged TTF–metal coordination polymer-based electron-rich framework with positively charged functional organic electron acceptors to form $\{[\text{cation}]^{n+} \cdot [\text{TTFs}]^{n-}\}$ IPCT-type complexes.

Here, we demonstrate the use of a TTF–tetracarboxylate–metal coordination anion and the organic photoactive methyl

Received: November 25, 2013

Published: March 12, 2014

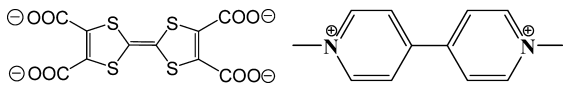
viologen dication¹² (a well-known electron acceptor, abbreviated as MV²⁺) (Chart 1) to organize the {[cation]ⁿ⁺}.


Chart 1. Structures of Tetrathiafulvalene–Tetracarboxylate L⁴⁻ (Left) and Methyl Viologen Dication MV²⁺ (Right)

{[TTF₈]ⁿ⁻} IPCT-type complexes, (MV)₂[Li₄(L)₂(H₂O)₆] (1), {(MV)(L)[Na₂(H₂O)₈·4H₂O]_n} (2), {(MV)[Mn(L)(H₂O)₂·2H₂O]_n} (3), and {(MV)[Mn(L)(H₂O)₂]_n} (4). The regular DADA mixed-stacking structures of these four compounds are characterized, and strong charge-transfer property is verified. It is known that the regular packing of donors and acceptors is a significant factor in obtaining photocurrent materials owing to excellent exciton separation and subsequent efficient electron transport to an electrode.¹³ Therefore, photocurrent responses of these compounds are investigated and discussed based on the metal coordination effects.

EXPERIMENTAL SECTION

General Remarks. The compound tetrathiafulvalene–tetracarboxylate sodium salt (Na₄L) was prepared using the method reported previously.^{9c} The compound tetrathiafulvalene–tetracarboxylate lithium salt (Li₄L) was obtained by following a similar procedure to that of Na₄L, but LiOH was used instead of NaOH. The IR spectra were recorded as KBr pellets on a Nicolet Magna 550 FT-IR spectrometer. Elemental analyses of C, H, and N were performed using an EA1110 elemental analyzer. ESR spectra were recorded on a Bruker ER-420 spectrometer with a 100 kHz magnetic field in X band at 110 K. Electronic absorption spectra were measured on a Shimadzu UV-3150 spectrometer. The temperature dependence of the magnetic susceptibility of a powdered sample was measured by a Quantum Design SQUID magnetometer on the MPMS-7 system. PXRD of compounds 1–4 were carried out on a D/MAX-3C X-ray diffraction meter with Cu Kα (λ = 1.5406 Å) radiation.

Preparation of Compounds. (MV)₂[Li₄(L)₂(H₂O)₆] (1). An aqueous solution (4 mL) of Li₄L (4.1 mg, 0.01 mmol) was mixed with a solution of MVI₂ (4.4 mg, 0.01 mmol) in DMF (4 mL). The mixed solution was stirred for 15 min at room temperature and filtered into a glass tube; then, dark blue crystals of 1 were obtained in 23 days from the filtrate by controlled evaporation of the solvent and were used for all measurements (2.3 mg, yield 19.1% based on Li₄L). Anal. Calcd for C₄₄H₄₀Li₄N₄O₂₂S₈: C, 41.91; H, 3.20; N, 4.44. Found: C, 41.85; H, 3.19; N, 4.33. IR data (cm⁻¹): 1623(vs), 1600(vs), 1536(m), 1434(w), 1337(vs), 1185(w), 1121(w), 1069(m), 833(m), 760(m).

{(MV)(L)[Na₂(H₂O)₈·4H₂O]_n} (2). Compound 2 was obtained by following a similar procedure to that of 1, but Na₄L (4.7 mg, 0.01 mmol) was used instead of Li₄L. Dark blue crystals of 2 were obtained in 20 days from the filtrate by controlled evaporation of the solvent and were used for all measurements (2.1 mg, yield 25.2% based on Na₄L). Anal. Calcd for C₂₂H₃₈N₂Na₂O₂₀S₄: C, 32.04; H, 4.64; N, 3.39. Found: C, 31.64; H, 3.80; N, 3.31. IR data (cm⁻¹): 1646(s), 1616(vs), 1589(s), 1430(w), 1335(s), 1162(w), 1109(w), 1075(m), 1001(w), 833(m), 760(m).

{(MV)[Mn(L)(H₂O)₂·2H₂O]_n} (3). An aqueous solution (6 mL) of Mn(OAc)₂·4H₂O (5.0 mg, 0.02 mmol) was added into the mixed solution of MVI₂ (4.4 mg, 0.01 mmol) in DMF (4 mL) and an aqueous solution (4 mL) of Li₄L (4.1 mg, 0.01 mmol). The final mixed solution was stirred for 15 min at room temperature and filtered into a glass tube; then, dark blue crystals of 3 were obtained in 10 days from the filtrate by controlled evaporation of the solvent and were used for all measurements (1.8 mg, yield 26.1% based on Li₄L). Anal. Calcd for C₂₂H₂₂MnN₂O₁₂S₄: C, 38.32; H, 3.22; N, 4.06. Found: C, 38.54; H,

3.19; N, 3.95. IR data (cm⁻¹): 1600(vs), 1584(vs), 1559(s), 1439(w), 1359(vs), 1223(w), 1092(w), 815(m), 738(m).

{(MV)[Mn(L)(H₂O)₂]_n} (4). Compound 4 was obtained by following a similar procedure to that of 3, but Na₄L (4.7 mg, 0.01 mmol) was used instead of Li₄L. Dark blue crystals of 4 were obtained in 20 days from the filtrate by controlled evaporation of the solvent and were used for all measurements (1.5 mg, yield 22.9% based on Na₄L). Anal. Calcd for C₂₂H₁₈MnN₂O₁₀S₄: C, 40.43; H, 2.78; N, 4.29. Found: C, 40.25; H, 2.65; N, 4.31. IR data (cm⁻¹): 1623(s), 1604(vs), 1579(s), 1559(s), 1434(w), 1355(vs), 1223(w), 1087(w), 815(m), 738(m).

X-ray Crystallographic Study. The measurement was carried out on a Rigaku Mercury CCD diffractometer at low temperature with graphite-monochromated Mo Kα (λ = 0.71073 Å) radiation. X-ray crystallographic data for all compounds were collected and processed using CrystalClear (Rigaku).¹⁴ The structure was solved by direct methods using SHELXS-97,¹⁵ and the refinement against all reflections of the compound was performed using SHELXL-97.¹⁶ All of the non-hydrogen atoms were refined anisotropically, and hydrogen atoms were added theoretically, except that the H atoms of O–H were located from the map. Relevant crystal data, collection parameters, and refinement results can be found in SI-Table 1.

Electrode Preparation and Photocurrent Measurement. The photoelectrodes of the compounds were prepared by the powder coating method. As a typical procedure, the crystals of compounds (0.005 mmol) were ground and pressed uniformly on the ITO glass (1.0 × 1.0 cm, 100 Ω/□). A 150 W high-pressure xenon lamp, located 20 cm away from the surface of the ITO electrode, was employed as a full-wavelength light source. The photocurrent experiments were performed on a CHI650E electrochemistry workstation in a three-electrode system, with the sample-coated ITO glass as the working electrode mounted on the window with an area of 1.0 cm², a Pt wire as auxiliary electrode, and a saturated calomel electrode (SCE) as reference electrode. The supporting electrolyte solution was a 0.1 mol·L⁻¹ sodium sulfate aqueous solution. The applied potential was 0.5 V for all measurements. The lamp was kept on continuously, and a manual shutter was used to block exposure of the sample to the light. The sample was typically irradiated at intervals of 20 s.

RESULTS AND DISCUSSION

Discussion of the Structures and Molecular Packings.

Since the charge-transfer and photoelectrochemical properties reported below were measured using crystal samples, the molecular structures are important to understand the properties and mechanism. Single crystals of the compounds were prepared carefully by controlled evaporation of the reaction solvents. X-ray structural analysis shows that compound 1 is composed of TTF–tetracarboxylate–alkali metal coordination anions and MV²⁺ cations. It consists of a tetranuclear unit crystallized in the triclinic $P\bar{1}$ space group. Two crystallographically equivalent Li(I)(2) atoms are linked together by carboxylate groups of the TTF moiety into a dinuclear unit, which are further joined to the other crystallographically different Li(I)(1) atom by a carboxylate group on the other side of the TTF moiety into a tetranuclear unit (Figure 1a and Figure S1a). The carboxyl groups of the two sides of the L⁴⁻ ligand exhibit different coordination modes: one is monodentate, and the other is μ_2 - η^2 - η^1 . There are strong hydrogen bond interactions between the tetranuclear units to form the column structure (Figure S1b, SI-Table 2). Compound 2 shows a supramolecular two-dimensional (2-D) structure, composed of MV²⁺ dications, the ligand L⁴⁻, and a one-dimensional (1-D) cationic [Na₂(H₂O)₈]_n²⁺ chain and crystallized in the monoclinic $P2_1/c$ space group. The NaI has a distorted octahedral environment, and the NaO6 octahedra are each edge-shared with two of its neighbors, forming a chain running along the *b*-axis with composition {Na₂(H₂O)₈]_n²⁺ (Figure S2).

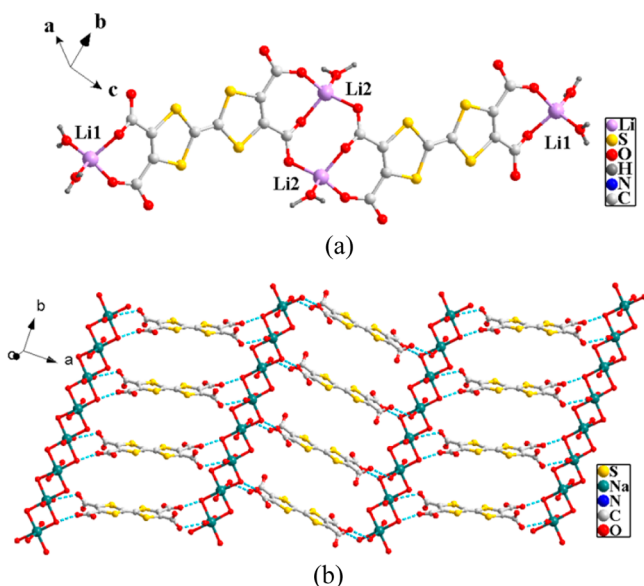


Figure 1. (a) Tetranuclear unit of compound 1; (b) two-dimensional supramolecular structure of compound 2. Hydrogen atoms were omitted for clarity.

The Na–O distances range from 2.346(6) to 2.444(5) Å. Every two carboxylate groups on two sides of the TTF moieties bridge neighboring Na–O chains through strong hydrogen bonds (SI-Table 2) to form a 2-D coordination network (Figure 1b). There is also strong hydrogen bonding among the cocrystallized water molecules and the oxygen atoms of carbonyl groups as well as the Na–O chains. The important bond lengths of the central double bonds of TTF moieties of 1 and 2 are 1.355(10) and 1.338(12) Å, respectively, and the

central double bonds of MV moieties of 1 and 2 are 1.471(10) and 1.477(12) Å, respectively, (discussed below). Details of the distances (Å) and angles (deg) of important bonds and C···C, C···S, and O···C contacts of 1 and 2 are given in the Supporting Information (SI-Table 3, SI-Table 4).

X-ray structural analysis shows that compounds 3 and 4 are composed of an anionic TTF–tetracarboxylate Mn(II) coordination polymer and MV²⁺ cations. The structure of 3 is crystallized in the monoclinic *C2/c* space group and consists of 1-D coordination chains (Figure 2a) and MV²⁺ cations. The Mn(II) ions are octahedrally coordinated by four carboxylate oxygen atoms from two different L⁴⁻ ligands and two coordinated water molecules at trans axial position (Figure S3) to form an infinite polymeric structure. Each carboxyl group of L⁴⁻ exhibits a monodentate binding manner, which is a new type of coordination mode found for the TTF–tetracarboxylate ligand.^{9c,d} The structure of compound 4 is crystallized in the monoclinic *P2₁/n* space group and is composed of a 2-D anionic [Mn(L)(H₂O)₂] network (Figure 2b) and MV²⁺ cations. There is only one crystallographically independent manganese atom, which is symmetrically coordinated by four carboxylate oxygen atoms from four different L⁴⁻ ligands and two coordinated water molecules at trans axial positions. The 2-D coordination network is achieved in the *ab*-plane by the Mn(II) coordination with the carboxylate groups on two sides of the TTF moieties with $\mu_4\text{-}\eta^1\text{:}\eta^1\text{:}\eta^1\text{:}\eta^1$ bridges (Figure S4). The important bond lengths of the central double bonds of TTF molecules of 3 and 4 are 1.310(10) and 1.342(11) Å, respectively, and the central double bonds of MV moieties of 3 and 4 are 1.488(11) and 1.461(13) Å, respectively (discussed below). The strong hydrogen bonding between the coordinated water molecules and the noncoordinated oxygen atoms of carbonyl groups appears to play a significant role in

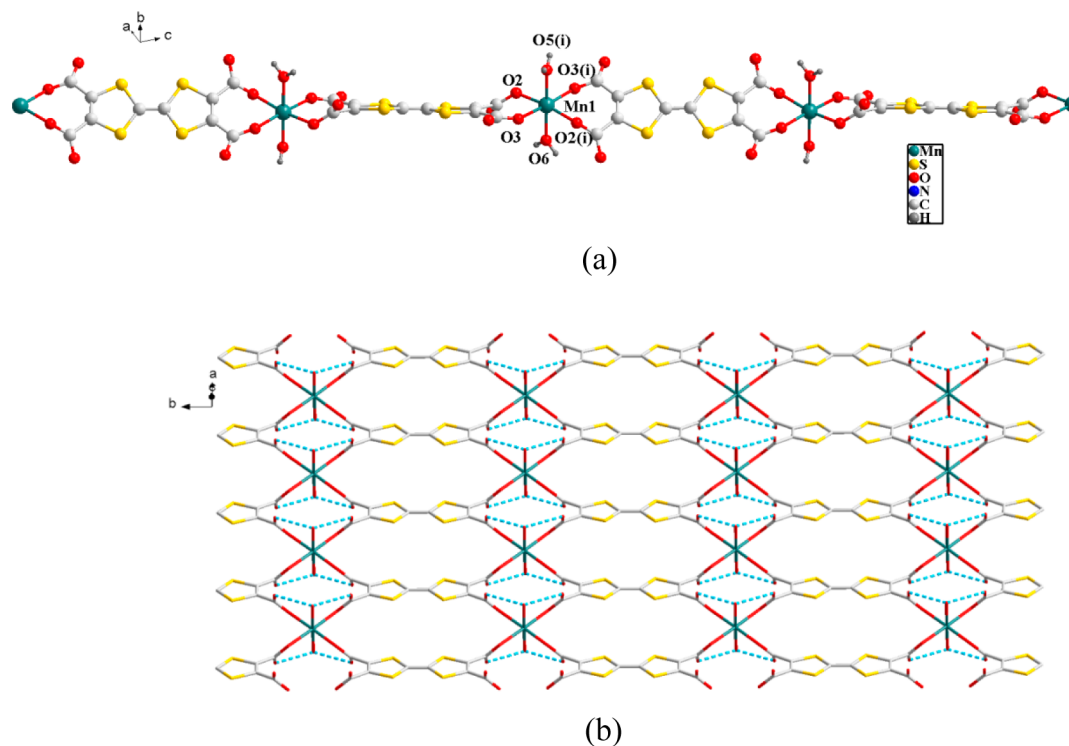


Figure 2. (a) Coordination 1-D chain bridged by L⁴⁻ ligands in 3 (i: 1–*x*, *y*, 0.5–*z*); (b) coordination 2-D regular network bridged by L⁴⁻ ligands of 4 (the sky blue dashed lines represent the hydrogen bonds). Hydrogen atoms were omitted for clarity.

the formation of the regular 2-D coordination networks (Figure 2b). Details of the distances (Å) and angles (deg) of important bonds, C⋯S and O⋯C contacts, and hydrogen bonds of **3** and **4** are given in the Supporting Information (SI-Table 2, SI-Table 3, SI-Table 4).

All the packing diagrams of the four compounds show that the electron donor TTF moiety and the electron acceptor MV²⁺ form a mixed-stack arrangement in alternating DADA fashion, as seen from Figure 3. In compounds **1–4**, the TTF moieties and the MV²⁺ cations are essentially parallel stacked, forming the columns with $\pi\cdots\pi$ stacking. The dihedral angles

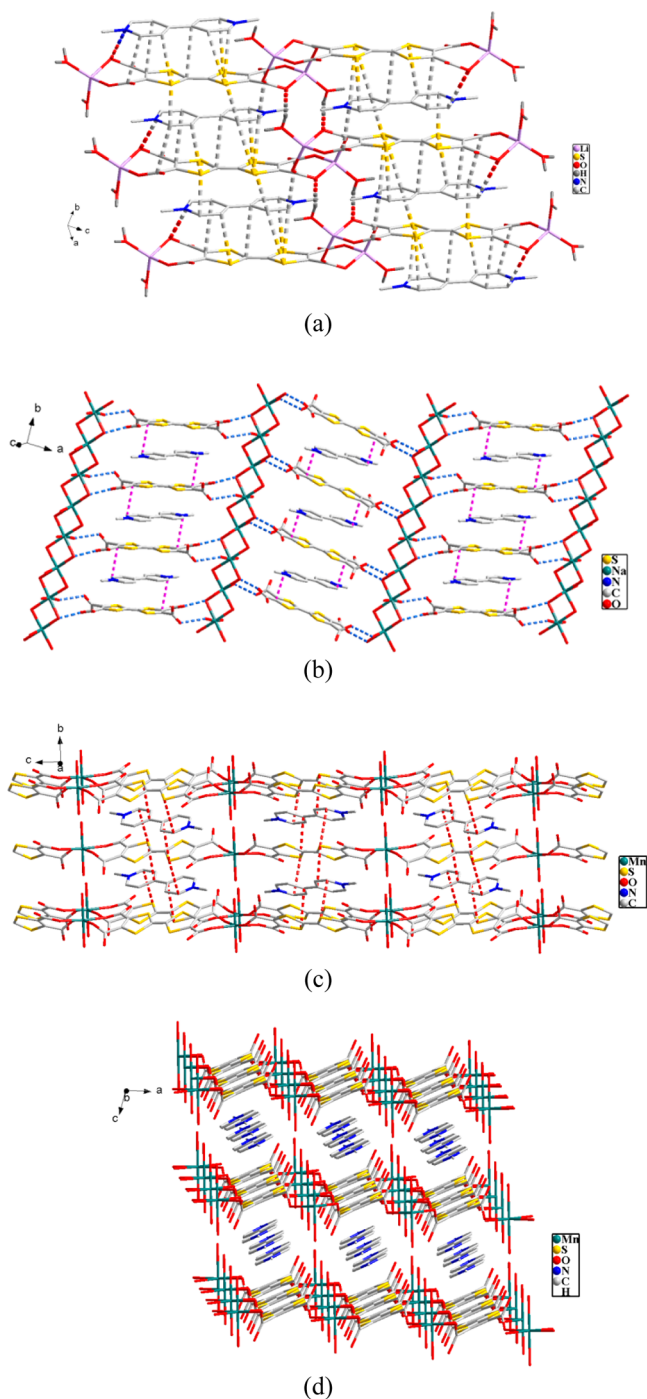


Figure 3. D–A packing diagrams of **1** (a), **2** (b), **3** (c), and **4** (d). Hydrogen atoms were omitted for clarity.

between the TTF mean plane (including two five-membered dithiolene rings) and the MV²⁺ mean plane (except two methyl groups) are 3.28(8)°, 2.21(10)°, 1.43(8)°, and 2.61(9)°, respectively. The distances between cation and anion planes are 3.30 Å for **1**, 3.45 Å for **2**, 3.40 Å for **3**, and 3.51 Å for **4**. The strong electrostatic interaction between the cation MV²⁺ and the anion is a main force that shortens the distances of the cation–anion pair. The TTF moiety in **1** is not a plane but with a dihedral angle between two five-membered dithiolene rings of 5.62(20)° and the bipyridinium moiety is also distorted with a dihedral angle between two pyridiniums of 4.99(24)°. The TTF moiety and MV²⁺ cation in **2**, **3**, and **4** are essentially planar with dihedral angles between two five-membered dithiolene rings of 0.00(21)°, 1.49(23)°, and 1.27(8)°, respectively, and the dihedral angle between two bipyridinium moieties of 0.00(34)°, 0.00(26)°, and 0.00(27)°, respectively. These stable and regular DADA-arranged structures may be of great concern regarding their physical properties.

Charge-Transfer Property. Although structural analysis for all four compounds gives details of the cation–anion arrangement and interactions, evidence of charge transfer should be verified by spectral measurement. In comparison with the red color of the neutral coordination polymer (denoted as [MTTFs]) of the same ligand,^{9c} the dark green color of the four salt crystals **1–4** (denoted as [MV]²⁺·[MTTFs]²⁻) (Figure 4) clearly suggests the possible occurrence of strong charge

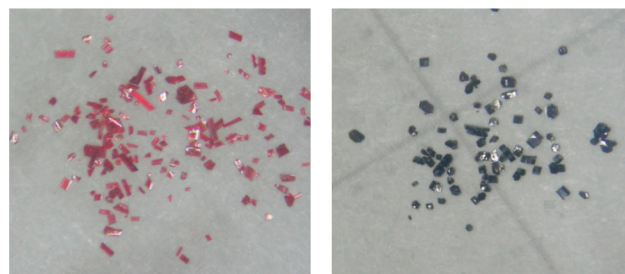


Figure 4. Color change from red [MTTFs] (left) to dark blue [MV]²⁺·[MTTFs]²⁻ (right).

transfer or electron transfer (the extreme case of charge transfer) between the cation and anion in the solid state. Optical diffuse-reflection spectra of **1–4** together with the starting materials MVI₂, Li₄L, and Na₄L were measured at room temperature using BaSO₄ as a standard reference. As shown in Figure 5, the spectra of **1–4** show a broad range of absorption

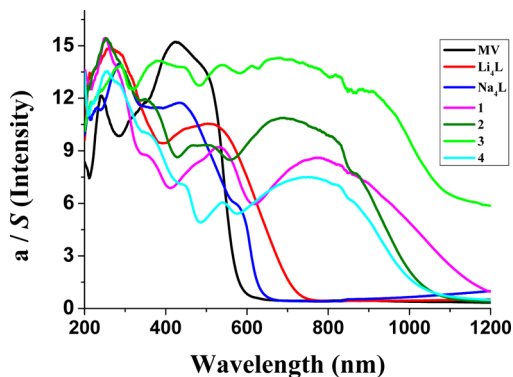


Figure 5. Electronic spectra of MVI₂, Li₄L, Na₄L, and **1–4** in the solid state.

in the visible and near-infrared range from about 600 to 950 nm. The new low-energy band is assigned to the absorption of charge transfer (CT) or partial electron transfer between the TTF anion and MV^{2+} cation. For comparison, no such band is observed for MV_2 , Li_4L , and Na_4L salts, and it is also different from the bands of $TTF^{\bullet+3d}$ and $MV^{\bullet+}$.^{12h} Clearly, the intense CT bands of 1–4 result from the cation and anion interaction, $\pi\cdots\pi$ interaction, and short contacts mentioned above.

Solution spectra of crystal 1 in different concentrations were measured (Figure S5). The peak at 720 nm (1.0×10^{-4} mol·L⁻¹) completely disappeared when the solution was 20 times diluted to 5.0×10^{-6} mol·L⁻¹. On the other hand, the frozen solution ESR spectrum (110 K) of 1 (1.0×10^{-2} mol·L⁻¹) is also silent for radical signal. All those results suggest that the low-energy band is a charge-transfer band (partial electron transfer in the ground state).

To investigate whether an efficient interion electron transfer has happened, ESR studies were carried out at 110 K (Figure 6). The ESR spectrum of compound 2 displays a sharp signal at

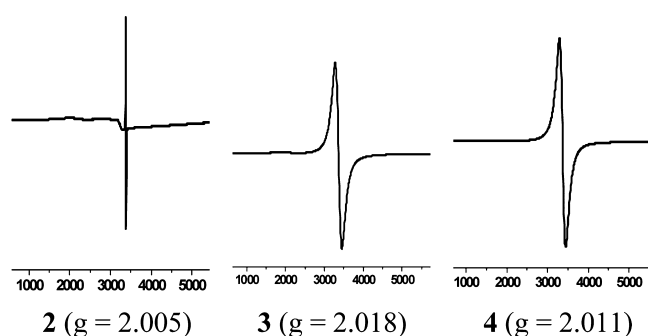


Figure 6. ESR spectra of 2–4 recorded at 110 K.

$g = 2.005$, which is in line with the characteristic ESR signal of the cation radical $TTF^{\bullet+17}$ and $MV^{\bullet+12h}$ units. The ESR spectra of compounds 3 and 4 show broadened signals with $g = 2.018$ and 2.011, respectively. In comparison with that of 2, the paramagnetic Mn(II) in 3 and 4 should be considered, and the broad signal includes the coupling of two resonance signals, the radicals of the $TTF^{\bullet+}$ and $MV^{\bullet+}$ units, and the unpaired electrons of the paramagnetic center of Mn(II) atom.

Combined the aforementioned structural results of the face-to-face DA packing modes with the existence of many interactions such as electrostatic interactions, $C\cdots C$ and $C\cdots S$ short contacts between TTF and MV moieties, the near-infrared CT bands, and the radical signals in the ESR spectra, we can conclude that there exist a strong charge transfer and even partial electron transfer from the TTF moiety to the MV^{2+} in all these ion pair compounds. However, although the charge transfer is very strong in these compounds, it should be noted that only some of the molecules are radicalized, because the bond lengths of the central double bonds of TTF molecules, being sensitive to oxidation, are 1.357(10), 1.338(12), 1.310(10), and 1.342(11) Å for 1–4, respectively, in the range of those reported for the TTF neutral state of the coordination compounds with the same ligand $L^{8e,9c,d}$ and shorter than those reported for the TTF radical cation (about 1.38–1.40 Å).¹⁸ The bond lengths of the C–S around the central double bonds (SI-Table 4) are also consistent with those reported for the TTF neutral state. Furthermore, according to the theoretical calculation, the largest changes in π charge density for the lowest-energy unoccupied orbital

(LUMO) in MV^{2+} in the transformation from MV^{2+} to $MV^{\bullet+}$ occur at the central C atoms, linking two pyridine rings, and N atoms.¹⁹ The Guo group reported that the bond distances of central C–C and N–C (represent as a and f or f' in SI-Table 4) are elongated by 0.04 and 0.018 Å.^{12a} The distances of these bonds for 1–4 are in the range of those reported in $MV(I_3)_2$.²⁰

Magnetic susceptibility measurement for complex 4 was performed on a SQUID magnetometer based on polycrystalline samples in the temperature range 2–300 K. The variation of the molar magnetic susceptibilities is shown as χ_m and $\chi_m T$ versus T plots in Figure S6. The $\chi_m T$ (5.70 cm³·K·mol⁻¹ at 300 K) gradually decreased when the temperature dropped, revealing the existence of antiferromagnetic interactions. The expected $\chi_m T$ value for an isolated $S = 5/2$ Mn(II) ion is 4.37 cm³·K·mol⁻¹, which is below the experimental 5.70 cm³·K·mol⁻¹. The result indicates that there is a magnetic contribution of the radical electrons, which is consistent with the result of the ESR measurement. The expected $\chi_m T$ value for the two isolated $S = 1/2$ radical electrons ($TTF^{\bullet+}$ and $MV^{\bullet+}$) and a $S = 5/2$ Mn(II) ion system is 5.125 ($= 4.375 + 0.375 \times 2$) cm³·K·mol⁻¹, smaller than the experimental value of 5.70 cm³·K·mol⁻¹, and is unreasonable for the system. Considering the conjugated structure of TTF with the metal center, the radical electron should not be an isolated one; therefore, it is difficult to estimate the extent of the electron transfer.

Photocurrent Response Property. The $[MV]^{2+}$ compounds are usually photo- or electroactive.¹² To investigate the photoelectric conversion properties of the $\{[MV]^{2+}, [MTTFs]^{2-}\}$ IPCT-type complexes, the photocurrent response experiments of 2, 3, and 4 were carried out with a three-electrode photoelectrochemical cell consisting of the sample modified ITO/CT-compound electrode (a more detailed description is given in the Experimental Section). Compound 1 has a large solubility in water. The data of compound 1 were not obtained. Usually, sacrificial reagents such as the electron acceptor viologen or electron donors triethanolamine and ascorbate are needed to be added into solution to generate a photocurrent.²¹ Complexes 1–4 are a coassembly of photoactive electron acceptor viologen and electron donor TTF and hence could be inherent photoelectron active materials. Therefore, the solution contains only 0.1 mol·L⁻¹ sodium sulfate as supporting electrolyte (in this system, water splitting may be involved in the electrode reaction).²² The results are shown in Figure 7 and Figure S7. Taking 4 as a representative (Figure 7a, red line), upon repetitive irradiation with xenon light on and off (interval 20 s), a clear photocurrent response was observed. The anodic photocurrent was reached quickly without delay and was stable without a decrease in the intensity, providing an effective and repeatable photocurrent response. The result demonstrates the reproducibility of the photoelectrode response and, hence, the mechanical and photo-physical stability of the electrode. The photocurrent response of complex 2 under the same experimental conditions is also displayed in Figure 7a (blue line). Comparing with those of 3 and 4, the current intensity of 2 is low, which seems to suggest that the Mn(II) ion or more exactly the coordination of the Mn(II) ion has an effect on the photocurrent response. PXRD patterns of compound 4 before and after the photocurrent experiment are shown in Figure S8, and they are essentially the same. Figure 7b shows the photocurrent response of compound 3 without light filter (red line), with a 380 nm light filter (blue line), and with a 420 nm light filter (green line). The current intensity decreases quickly when the cut wavelength increases.

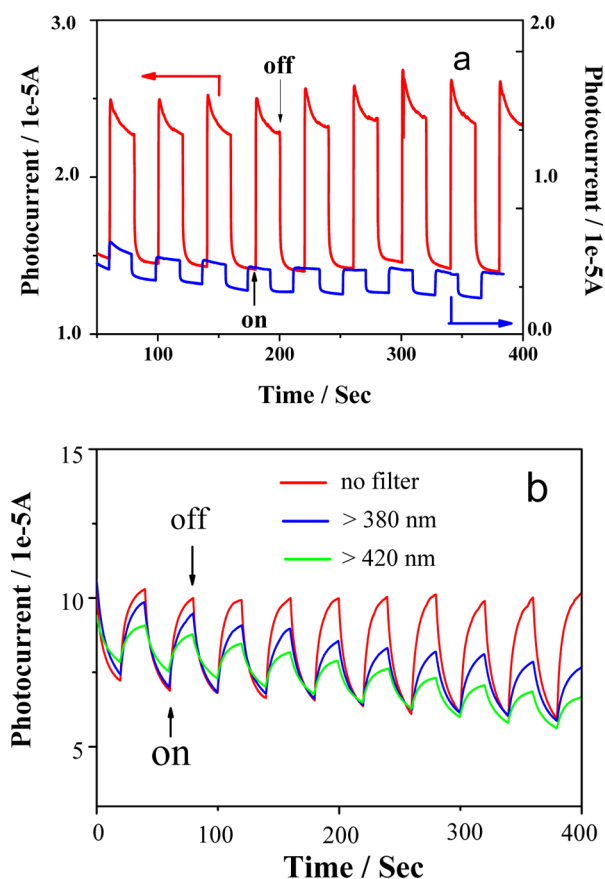


Figure 7. (a) Photocurrent responses of **2** (blue line) and **4** (red line) in the presence of a $0.1 \text{ mol}\cdot\text{L}^{-1}$ Na_2SO_4 aqueous solution, irradiated by a full-wavelength band high-pressure xenon lamp. (b) Photocurrent responses of **3** without light filter (red line), with a 380 nm light filter (blue line), and with a 420 nm light filter (green line).

Although compounds **3** and **4** are similar, the coordination modes, the structural dimensions, and the interactions between cations and anions are different. All the factors may affect the shape and the intensity of the photocurrent response.

The proposed electron-transfer route for the observed large anodic photocurrent for the $\{[\text{MV}]^{2+}\cdot[\text{MTTFs}]^{2-}\}/\text{ITO}$ electrode is shown in Figure 8. First, upon irradiation, the

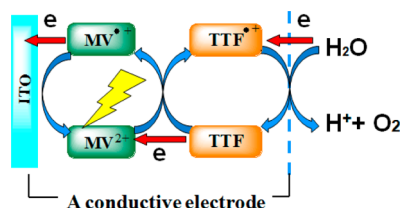


Figure 8. Photocurrent generation diagram including the electron flow.

photosensitive MV^{2+} ion is excited to form the $\text{MV}^{\bullet+}$ radical with the cooperative electron transfer from the TTF donor to the MV^{2+} ion. Then the $\text{MV}^{\bullet+}$ radical transfers the electron to the ITO electrode and returns to the MV^{2+} ion. The TTF moiety loses one electron to form the $\text{TTF}^{\bullet+}$ radical and generates the electron conductive pair of $\text{TTF}^{\bullet+}\cdot\text{MV}^{\bullet+}$. The conductive solid-state intermediate ensures the effective electron flow in the crystals.

Why can the $[\text{MV}]^{2+}\cdot[\text{MnTTFs}]^{2-}/\text{ITO}$ electrodes increase the current intensity in comparison with that of the $[\text{MV}]^{2+}\cdot[\text{NaTTFs}]^{2-}/\text{ITO}$ electrodes? Two aspects may be considered for understanding the photocurrent behavior. The first one involves the $\text{Mn(III)}/\text{Mn(II)}$ redox couple. The $\text{TTF}^{\bullet+}$ obtains an electron from the Mn(II) center and returns to a neutral TTF state. The formed Mn(III) reacts with water²³ to complete the electrode reactions, which can explain the effective photocurrent response of TTF–Mn compounds. The water molecules act in the function of the sacrificial reagent. The second one involves the effective electron transfer between the electron donor TTF moiety and the electron acceptor MV^{2+} moiety. The alternating DADA arrangement of the TTF moiety and viologen molecule is found in the packing of all four ion pair compounds. The distances between the cation and anion planes are about 3.45, 3.40, and 3.51 Å for compounds **2–4**, respectively, which shows no obvious relationship to the photocurrent intensity. Figure 9 shows the

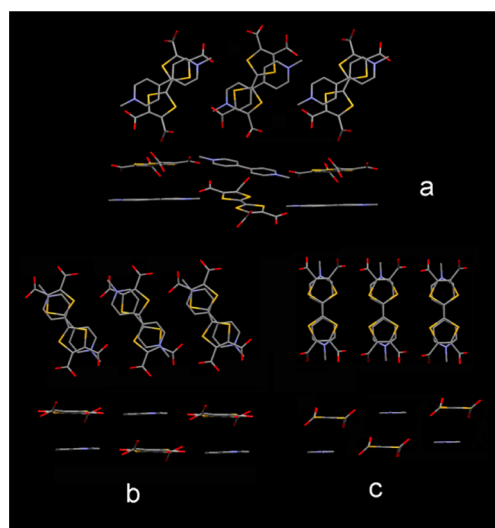


Figure 9. Dimer packing of the three compounds viewed on the top and side of **2** (a), **3** (b), and **4** (c).

dimer packing of the three compounds viewed on the top and side. It is obvious that the donor and acceptor moieties in **3** and **4** are stacked effectively and regularly, while only some of the D and A planes are stacked and there are two orientations in **2**. Therefore, the effective face-to-face D–A arrangement in Mn(II) coordination polymers might be another possible reason for the higher photocurrent response.¹³ The effective arrangement is due to the metal–ligand coordination that fixes the space between the TTF moiety and the MV^{2+} ion. Anyway, the details of the mechanism should be verified by further experiments and theoretical studies.

CONCLUSIONS

Compounds **1–4**, $(\text{MV})_2[\text{Li}_4(\text{L})_2(\text{H}_2\text{O})_6]$ (**1**), $\{(\text{MV})\cdot[\text{Na}_4(\text{L})(\text{OH})_2(\text{H}_2\text{O})_6]\cdot 2\text{H}_2\text{O}\}_n$ (**2**), $\{(\text{MV})[\text{Mn}(\text{L})(\text{H}_2\text{O})_2]\cdot 2\text{H}_2\text{O}\}_n$ (**3**), and $\{(\text{MV})[\text{Mn}(\text{L})(\text{H}_2\text{O})_2]\}_n$ (**4**), are the first examples of $\{[\text{cation}]^{n+}\cdot[\text{TTFs}]^{n-}\}$ IPCT-type salts. In these salts, the functional organic cation, photoactive methyl viologen, is introduced into the TTF–metal coordination polymer. Single-crystal X-ray structural analysis of the four compounds shows that the electron donor and the electron acceptor form a regular mixed-stack arrangement in alternating

DADA fashion. The strong electrostatic interaction plays an important role in shortening the distance between the cation and anion planes, which is in favor of the cation–anion charge transfer in all these complexes. These MV–TTF compounds possess an effective and repeatable photocurrent responsive property. The coordination center of the Mn(II) ion has a great effect on the increasing photocurrent response. Usually, sacrificial reagents like the electron acceptor viologen are needed to be added into solution to generate a photocurrent. Complexes 1–4 are an inherent coassembly of the photoactive electron acceptor viologen and the electron donor TTF and hence could be viable materials for photoelectronics.

■ ASSOCIATED CONTENT

■ Supporting Information

Crystal data and structural refinement parameters for 1–4; description of the structures; the coordination environment of Li1 and Li2 of 1; hydrogen bond interactions between the tetranuclear units; the coordination environment of Na1 and Na2 of 2; the 2-D anionic $[\text{Na}_4(\text{L})(\text{OH})_2(\text{H}_2\text{O})_6]$ network formed by Na–O chains and L; the coordination 1-D chain bridged by L^{4-} ligands in 3 (i: 1–x, y, 0.5–z); the coordination 2-D regular network bridged by L^{4-} ligands of 4; experimental χ_m versus T and $\chi_m T$ versus T curves for complex 4; photocurrent responses of 3 in the presence of a 0.1 mol·L⁻¹ Na₂SO₄ aqueous solution. This material is available free of charge via the Internet at <http://pubs.acs.org>.

■ AUTHOR INFORMATION

Corresponding Authors

*E-mail: zhuqinyu@suda.edu.cn.

*E-mail: daijie@suda.edu.cn.

Notes

The authors declare no competing financial interest.

■ ACKNOWLEDGMENTS

We gratefully acknowledge financial support by the NSF of China (21171127), the Priority Academic Program Development of Jiangsu Higher Education Institutions, and the Program of Innovative Research Team of Soochow University.

■ REFERENCES

- (1) (a) Salinas, Y.; Martínez-Máñez, R.; Marcos, M. D.; Sancenón, F.; Costero, A. M.; Parra, M.; Gil, S. *Chem. Soc. Rev.* **2012**, *41*, 1261–1296. (b) Zhao, Y.; Liang, W. *Chem. Soc. Rev.* **2012**, *41*, 1075–1087. (c) Shimomura, S.; Kitagawa, S. *J. Mater. Chem.* **2011**, *21*, 5537–5546. (d) Piliego, C.; Loi, M. A. *J. Mater. Chem.* **2012**, *22*, 4141–4150. (e) Mori, T.; Terasaki, I.; Mori, H. *J. Mater. Chem.* **2007**, *17*, 4343–4347. (f) Peng, H.; Liu, Z. *Coord. Chem. Rev.* **2010**, *254*, 1151–1168.
- (2) Ferraris, J. P.; Cowan, D. O.; Walatka, V.; Perlstein, J. H. *J. Am. Chem. Soc.* **1973**, *95*, 948–949.
- (3) (a) Yamada, J.; Sugimoto, T. *TTF Chemistry: Fundamentals and Application of Tetrathiafulvalene*; Springer: Berlin, 2004. (b) Kimura, S.; Suzuki, H.; Maejima, T.; Mori, H.; Yamaura, J.-I.; Kakiuchi, T.; Sawa, H.; Moriyama, H. *J. Am. Chem. Soc.* **2006**, *128*, 1456–1457. (c) Iimori, T.; Naito, T.; Ohta, N. *J. Phys. Chem. C* **2010**, *114*, 9070–9075. (d) Iimori, T.; Sabeth, F.; Naito, T.; Ohta, N. *J. Phys. Chem. C* **2011**, *115*, 23998–24003. (e) Shen, C. K.-F.; Duong, H. M.; Sonmez, G.; Wudl, F. *J. Am. Chem. Soc.* **2003**, *125*, 16206–16207.
- (4) See for example: (a) Bryce, M. R. *Adv. Mater.* **1999**, *11*, 11–23 and references therein. (b) Segura, J. L.; Martín, N. *Angew. Chem.* **2001**, *113*, 1416–1455; *Angew. Chem., Int. Ed.* **2001**, *40*, 1372–1409 and references therein. (c) Simonsen, K. B.; Zong, K.; Rogers, R. D.; Cava, M. P.; Becher, J. *J. Chem. Commun.* **1997**, *62*, 679–686. (d) Simonsen,

- K. B.; Thorup, N.; Cava, M. P.; Becher, J. *Chem. Commun.* **1998**, 901–902. (e) Perepichka, D. F.; Bryce, M. R.; McInnes, E. J. L.; Zhao, J. *Org. Lett.* **2001**, *3*, 1431–1434. (f) Metzger, R. M. *Acc. Chem. Res.* **1999**, *32*, 950–957. (g) Metzger, R. M.; Chen, B.; Höpfner, U.; Lakshmikantham, M. V.; Vuillaume, D.; Kawai, T.; Wu, X.; Tachibana, H.; Hughes, T. V.; Sakurai, H.; Baldwin, J. W.; Hosch, C.; Cava, M. P.; Brehmer, L.; Ashwell, G. J. *J. Am. Chem. Soc.* **1997**, *119*, 10455–10466. (h) Dumur, F.; Gautier, N.; Gallego-Planas, N.; Sahin, Y.; Levillain, E.; Mercier, N.; Hudhomme, P.; Masino, M.; Girlando, A.; Lloveras, V.; Vidal-Gancedo, J.; Veciana, J.; Rovira, C. *J. Org. Chem.* **2004**, *69*, 2164–2177. (i) Mei, X.; Ouyang, J. *Langmuir* **2011**, *27*, 10953–10961. (j) Jia, H.; Schmid, B.; Liu, S.-X.; Jaggi, M.; Monbaron, P.; Bhosale, S. V.; Rivadehi, S.; Langford, S. J.; Sanguinet, L.; Levillain, E.; El-Khouly, M. E.; Morita, Y.; Fukuzumi, S.; Decurtins, S. *ChemPhysChem* **2012**, *13*, 3370–3382. (k) Guasch, J.; Grisanti, L.; Souto, M.; Lloveras, V.; Vidal-Gancedo, J.; Ratera, I.; Painelli, A.; Rovira, C.; Veciana, J. *J. Am. Chem. Soc.* **2013**, *135*, 6958–6967.

(5) See for example: (a) Nielsen, M. B.; Lomholt, C.; Becher, J. *Chem. Soc. Rev.* **2000**, *29*, 153–164. (b) Nielsen, K. A.; Jeppesen, J. O.; Levillain, E.; Becher, J. *Angew. Chem., Int. Ed.* **2003**, *42*, 187–191. (c) Wang, Z.; Zhang, D.; Zhu, D. *J. Org. Chem.* **2005**, *70*, 5729–5732. (d) Lu, H.; Xu, W.; Zhang, D.; Chen, C.; Zhu, D. *Org. Lett.* **2005**, *7*, 4629–4632. (e) Lu, H.; Xu, W.; Zhang, D.; Zhu, D. *Chem. Commun.* **2005**, 4777–4779. (f) Nielsen, K. A.; Cho, W.-S.; Lyskawa, J.; Levillain, E.; Lynch, V. M.; Sessler, J. L.; Jeppesen, J. O. *J. Am. Chem. Soc.* **2006**, *128*, 2444–2451. (g) Liu, W.; Lu, J.-H.; Ji, Y.; Zuo, J.-L.; You, X.-Z. *Tetrahedron Lett.* **2006**, *47*, 3431–3434. (h) Dolder, S.; Liu, S.-X.; Le Derf, F.; Sallé, M.; Neels, A.; Decurtins, S. *Org. Lett.* **2007**, *9*, 3753–3756. (i) Jia, H.-P.; Forgie, J. C.; Liu, S.-X.; Sanguinet, L.; Levillain, E.; Le Derf, F.; Sallé, M.; Neels, A.; Skabara, P. J.; Decurtins, S. *Tetrahedron* **2012**, *68*, 1590–1594.

(6) Bigoli, F.; Deplano, P.; Mercuri, M. L.; Pellinghelli, M. A.; Pilia, L.; Pintus, G.; Serpe, A.; Trogu, E. F. *Inorg. Chem.* **2002**, *41*, 5241.

(7) (a) Kurmoo, M.; Bonamico, M.; Bellitto, C.; Fares, V.; Federici, F.; Guionneau, P.; Ducasse, L.; Kitagawa, H.; Day, P. *Adv. Mater.* **1998**, *10*, 545–550. (b) Avarvari, N.; Fourmigué, M. *Chem. Commun.* **2004**, 1300–1301. (c) Li, Q.; Lu, J.; Boas, J. F.; Traore, D. A. K.; Wilce, M. C. J.; Huang, F.; Martin, L. L.; Ueda, T.; Bond, A. M. *Inorg. Chem.* **2012**, *51*, 12929–12937. (d) Saito, G.; Hosoda, H.; Yoshida, Y.; Hagiwara, J.; Nishimura, K.; Yamochi, H.; Otsuka, A.; Hiramatsu, T.; Shimazaki, Y.; Kiracki, K.; Cordier, S.; Perrin, C. *J. Mater. Chem.* **2012**, *22*, 19774–19791. (e) Kurmoo, M.; Graham, A. W.; Day, P.; Coles, S. J.; Hursthouse, M. B.; Caulfield, J. L.; Singleton, J.; Pratt, F. L.; Hayes, W.; Ducasse, L.; Guionneau, P. *J. Am. Chem. Soc.* **1995**, *117*, 12209–12217. (f) Lu, W.; Zhu, Q. Y.; Dai, J.; Zhang, Y.; Bian, G. Q.; Liu, Y.; Zhang, D. Q. *Cryst. Growth Des.* **2007**, *7*, 652. (g) Fourmigué, M.; Reinheimer, E. W.; Assaf, A.; Jeannin, O.; Saad, A. *Inorg. Chem.* **2011**, *50*, 4171–4181.

(8) (a) Ebihara, M.; Nomura, M.; Sakai, S.; Kawamura, T. *Inorg. Chim. Acta* **2007**, *360*, 2345–2352. (b) Pointillart, F.; Gal, Y. L.; Golhen, S.; Cador, O.; Ouahab, L. *Chem. Commun.* **2009**, 3777–3779. (c) Chen, Y.; Li, C.; Wang, C.; Wu, D.; Zuo, J.; You, X. *Sci. China, B* **2009**, *52*, 1596–1601. (d) Han, Y.-F.; Li, X.-Y.; Li, J.-K.; Zheng, Z.-B.; Wu, R. T.; Lu, J.-R. *Chin. J. Inorg. Chem.* **2009**, *25*, 1290–1294. (e) Nguyen, T. L. A.; Devic, T.; Mialane, P.; Rivière, E.; Sonnauer, A.; Stock, N.; Demir-Cakan, R.; Morcrette, M.; Livage, C.; Marrot, J.; Tarascon, J.-M.; Férey, G. *Inorg. Chem.* **2010**, *49*, 10710–10717.

(9) (a) Gu, J.; Zhu, Q.-Y.; Zhang, Y.; Lu, W.; Niu, G.-Y.; Dai, J. *Inorg. Chem. Commun.* **2008**, *11*, 175–178. (b) Zhu, Q.-Y.; Wang, J.-P.; Qin, Y.-R.; Shi, Z.; Han, Q.-H.; Bian, G.-Q.; Dai, J. *Dalton Trans.* **2011**, *40*, 1977–1983. (c) Qin, Y.-R.; Zhu, Q.-Y.; Huo, L.-B.; Shi, Z.; Bian, G.-Q.; Dai, J. *Inorg. Chem.* **2010**, *49*, 7372–7381. (d) Shao, M.-Y.; Huo, P.; Sun, Y.-G.; Li, X.-Y.; Zhu, Q.-Y.; Dai, J. *CrystEngComm* **2013**, *13*, 1086–1094.

(10) Nguyen, T. L. A.; Demir-Cakan, R.; Devic, T.; Morcrette, M.; Ahnfeldt, T.; Auban-Senzier, P.; Stock, N.; Goncalves, A.-M.; Filinchuk, Y.; Tarascon, J.-M.; Férey, G. *Inorg. Chem.* **2010**, *49*, 7135–7143.

(11) Wang, J.-P.; Lu, Z.-J.; Zhu, Q.-Y.; Zhang, Y.-P.; Qin, Y.-R.; Bian, G.-Q.; Dai, J. *Cryst. Growth Des.* **2010**, *10*, 2090–2095.

(12) (a) Xu, G.; Guo, G.; Wang, M.; Zhang, Z.; Chen, W.; Huang, J. *Angew. Chem., Int. Ed.* **2007**, *46*, 3249–3251. (b) Leblanc, N.; Bi, W.; Mercier, N.; Auban-Senzier, P.; Pasquier, C. *Inorg. Chem.* **2010**, *49*, 5824–5833. (c) Sagade, A. A.; Rao, K. V.; George, S. J.; Dattac, A.; Kulkarni, G. U. *Chem. Commun.* **2013**, *49*, 4847–5849. (d) Ye, H.; Park, H. S.; Akhavan, V. A.; Goodfellow, B. W.; Panthani, M. G.; Korgel, B. A.; Bard, A. J. *J. Phys. Chem. C* **2011**, *115*, 234–240. (e) Tapley, A.; Vaccarello, D.; Hedges, J.; Jia, F.; Love, D. A.; Ding, Z. *Phys. Chem. Chem. Phys.* **2013**, *15*, 1431–1436. (f) Manocchi, A. K.; Baker, D. R.; Pendley, S. S.; Nguyen, K.; Hurley, M. M.; Bruce, B. D.; Sumner, J. J.; Lundgren, C. A. *Langmuir* **2013**, *29*, 2412–2419. (g) Matsuuo, Y.; Ichiki, T.; Radhakrishnan, S. G.; Guldi, D. M.; Nakamura, E. *J. Am. Chem. Soc.* **2010**, *132*, 6342–6348. (h) Lin, R.-G.; Xu, G.; Wang, M.-S.; Lu, G.; Li, P.-X.; Guo, G.-C. *Inorg. Chem.* **2013**, *52*, 1199–1205.

(13) (a) Li, W.; Yamamoto, Y.; Fukushima, T.; Saeki, A.; Seki, S.; Tagawa, S.; Masunaga, H.; Sasaki, S.; Takata, M.; Aida, T. *J. Am. Chem. Soc.* **2008**, *130*, 8886–8887. (b) Naito, T.; Karasudani, T.; Mori, S.; Ohara, K.; Konishi, K.; Takano, T.; Takahashi, Y.; Inabe, T.; Nishihara, S.; Inoue, K. *J. Am. Chem. Soc.* **2012**, *134*, 18656–18666.

(14) *CrystalClear Software User's Guide*; Rigaku Corporation, 1999. Pflugrath, J. W. *Acta Crystallogr. Sect. D* **1999**, *55*, 1718–1725.

(15) Sheldrick, G. M. *SHELXS-97, Program for Structure Solution*; Universität of Göttingen: Germany, 1999.

(16) Sheldrick, G. M. *SHELXL-97, Program for Structure Refinement*; Universität of Göttingen: Germany, 1997.

(17) (a) Berridge, R.; Skabara, P. J.; Pozo-Gonzalo, C.; Kanibolotsky, A.; Lohr, J.; McDouall, J. J. W.; McInnes, E. J. L.; Wolowska, J.; Winder, C.; Sariciftci, N. S.; Harrington, R. W.; Clegg, W. *J. Phys. Chem. B* **2006**, *110*, 3140–3152. (b) Gomar-Nadal, E.; Mugica, L.; Vidal-Gancedo, J.; Casado, J.; Navarrete, J. T. L.; Veciana, J.; Rovira, C.; Amabilino, D. B. *Macromolecules* **2007**, *40*, 7521–7531.

(18) Boudiba, L.; Gouasmia, A.; Golhen, S.; Ouahab, L. *Synth. Met.* **2011**, *161*, 1800–1804.

(19) Prout, C. K.; Murray-Rust, P. *J. Chem. Soc. A* **1969**, 1520–1524.

(20) (a) Garcia, M. D.; Marti-Rujas, J.; Metrangolo, P.; Peinador, C.; Pilati, T.; Resnati, G.; Terraneo, G.; Ursini, M. *CrystEngComm* **2011**, *13*, 4411–4416. (b) Hu, T. *Acta Crystallogr., Sect. E (Struct. Rep. Online)* **2009**, *65*, o1162.

(21) (a) Yasutomi, S.; Morita, T.; Kimura, S. *J. Am. Chem. Soc.* **2005**, *127*, 14564–14565. (b) Driscoll, P. F.; Douglass, E. F.; Phewluangdee, M., Jr.; Soto, E. R.; Cooper, C. G. F.; MacDonald, J. C.; Lambert, C. R.; McGimpsey, W. G. *Langmuir* **2008**, *24*, 5140–5145. (c) Matsuoka, K.; Akiyama, T.; Yamada, S. *J. Phys. Chem. C* **2008**, *112*, 7015–7020. (d) Xue, P.; Lu, R.; Zhao, L.; Xu, D.; Zhang, X.; Li, K.; Song, Z.; Yang, X.; Takafuji, M.; Ihara, H. *Langmuir* **2010**, *26*, 6669–6675. (e) Trammell, S. A.; Dressick, W. J.; Melde, B. J.; Moore, M. J. *Phys. Chem. C* **2011**, *115*, 13446–13461. (f) Liu, L.; Zhan, W. *Langmuir* **2012**, *28*, 4877–4882. (g) Zhu, M.; Dong, Y.; Xiao, B.; Du, Y.; Yang, P.; Wang, X. *J. Mater. Chem.* **2012**, *22*, 23773–23779.

(22) (a) Higashi, M.; Domen, K.; Abe, R. *J. Am. Chem. Soc.* **2012**, *134*, 6968–6971. (b) Hill, J. C.; Choi, K.-S. *J. Phys. Chem. C* **2012**, *116*, 7612–7620.

(23) (a) Liu, X.; Wang, F. *Cood. Chem. Rev.* **2012**, *256*, 1115–1136. (b) Najafpour, M. M.; Ehrenberg, T.; Wiechen, M.; Kurz, P. *Angew. Chem.* **2010**, *122*, 2281–2285; *Angew. Chem., Int. Ed.* **2010**, *49*, 2233–2237. (c) Nepal, B.; Das, S. *Angew. Chem.* **2013**, *125*, 7365–7368; *Angew. Chem., Int. Ed.* **2013**, *52*, 7224–7227.